

A Perturbation Approach for Approximate Inertial Manifolds

Dongjin Kim

*Division of Integrated BioDefense
ISIS Center, Georgetown University
Washington, DC 20057, U.S.A
E-mail: dkim@isis.georgetown.edu*

Firdaus E. Udvardia

*Aerospace and Mechanical Engineering, Civil Engineering, Mathematics,
Systems Architecture Engineering, and Information and Operations Management
University of Southern California
Los Angeles, CA 90089-1453, U.S.A*

Wlodek Proskurowski

*Department of Mathematics
University of Southern California
Los Angeles, CA 90089, U.S.A*

Abstract

We present an explicit form for the construction of approximate inertial manifolds (AIMs) for a class of nonlinear dissipative partial differential equations by using a perturbation technique. We investigate two numerical examples of the reaction diffusion equation with polynomial nonlinearity and non-polynomial nonlinearity to show comparison of accuracy for our perturbation method with other well-known nonlinear Galerkin methods such as Foias-Manley-Temam and Euler-Galerkin methods. The proposed method for obtaining approximate inertial manifolds, though computationally more expensive, provides superior accuracy when compared with other AIM methods currently in use.

1. Introduction

The aim of this paper is to present an explicit form for the construction of approximate inertial manifolds (AIMs) for a class of nonlinear dissipative partial differential equations by using a perturbation technique.

An inertial manifold is a finite-dimensional, exponentially attracting, positively invariant Lipschitz manifold. Partial differential equations can be treated as infinite-dimensional dynamical systems on a suitable Hilbert space. For certain classes of dissipative dynamical systems [1] (see examples therein) inertial manifold theory allows for the reduction of the infinite-dimensional dynamics to a finite-dimensional system of ordinary differential equations referred to as inertial form which shares all the long term dynamics of the original problem [2], [3].

Existence results of inertial manifolds can be found in Foias, Sell, and Temam [3] and Mallet-Paret and Sell [4] (see the references therein). However, there are still many dissipative partial differential equations for which the existence of inertial manifolds is not known [5]. Foias, Manly and Temam [6] have introduced the concept of approximate inertial manifolds in the case of the two-dimensional Navier-Stokes equations for which the existence of an inertial manifold is not known.

From a practical point of view, approximate inertial manifolds can be applied regardless of the existence of an actual inertial manifold. They are useful because detailed simulations, stability and bifurcation calculations can be performed on the inertial form at a small fraction of the computational effort required to perform them on large-scale discretizations of the original equations. And systems for which such calculations could be prohibitively expensive may become tractable by using approximate inertial manifolds. [7]

The nonlinear evolutionary equation which we will study has the form

$$\frac{du}{dt} + Au + F(u) = 0, \quad (1.1)$$

where A , with the appropriate boundary condition (Dirichlet, Neumann, periodic), is a suitable linear, unbounded, self-adjoint and positive operator on a suitable Hilbert space H with dense domain $D(A) \subset H$, while F is nonlinear operator and the nonlinear term $F(u)$ can be approximated by Taylor's series (detail is later). Suppose further that A^{-1} is compact. As a result, eigenfunctions of the operator A , $\{e_j\}_{j=1}^{\infty}$, with corresponding eigenvalues $0 < \lambda_1 \leq \lambda_2 \leq \dots$, form a complete orthonormal basis in H . Let us denote P the orthogonal projection onto the span of the first N_p eigenfunctions $\{e_1, e_2, \dots, e_{N_p}\}$ and let $Q = I - P$.

If $u = u(x, t)$ is a solution of (1.1) we define $p = p(x, t)$ and $q = q(x, t)$ by $p = Pu$ and $q = Qu$. By projection of (1.1) on PH and QH , we find that p and q are solutions of the coupled system of equations

$$\frac{dp}{dt} + Ap + PF(p + q) = 0, \quad (1.2)$$

$$\frac{dq}{dt} + Aq + QF(p + q) = 0, \quad (1.3)$$

where $Ap = APu = PAu$ and $Aq = AQu = QAu$.

The standard Galerkin approximation of (1.1) using N_p modes can be expressed by setting $q = 0$ in (1.2), i.e.,

$$\frac{dp}{dt} + Ap + PF(p) = 0. \quad (1.4)$$

Instead, nonlinear Galerkin methods which are based on approximate inertial manifolds (AIM) such as those introduced by Foias, Manley, and Temam [6], the Euler-Galerkin AIM introduced by Foias, Sell, and Titi [8] approximate $u = p + \Phi_{\text{app}}$, where p satisfies the inertial form

$$\frac{dp}{dt} + Ap + PF(p + \Phi_{\text{app}}) = 0, \quad (1.5)$$

and each Φ_{app} is defined by

$$\Phi_{\text{app}}(p) = \begin{cases} -A^{-1}QF(p) & \text{FMT AIM} \\ -\tau(I + \tau AQ)^{-1}QF(p) & \text{Euler-Galerkin AIM} \end{cases} \quad (1.6)$$

choosing τ comparable to $\lambda_{N_p}^{-1}$ [8]. Several functions Φ_{app} have been introduced in [3], [5], [9], [10].

In this paper we will be looking for a better approximate inertial manifold by using a perturbation technique. Our approximate inertial manifold will be constructed by a modification of the perturbation result for numerical purposes. The perturbation result is expressed explicitly as a finite sum which is an approximate solution of the perturbed equation obtained from the equation (1.3).

This paper is organized as follows: In section 2, we present a finite series for an approximate solution of q in (1.3) by using a perturbation technique. And we construct a sequence of approximate inertial manifolds by modification of this perturbation result. In section 3, we investigate two numerical examples of the reaction diffusion equation with polynomial and non-polynomial nonlinearities. We show better accuracy of our perturbation method compared with other well-known nonlinear Galerkin methods. In section 4, we summarize the advantages and disadvantages of our perturbation method for the construction of approximate inertial manifolds.

2. Approximate inertial manifold with perturbation technique

This section has two parts. In the first part we introduce the perturbed equation from the q -equation (1.3) by defining a small positive parameter ϵ . Then we obtain the approximate solution of q in the form of an explicit finite sum by using a perturbation technique. In the second part we modify the previous result for numerical purposes to construct a sequence of approximate inertial manifolds.

2.1. Perturbation technique

Let us define a small positive number $\epsilon = 1/\lambda_{N_p+1}$ and the operator ϵA on $QD(A)$ as the linear operator L . Then the linear operator L is constant order with respect to ϵ , that is,

$$Lq = \epsilon Aq \sim \mathcal{O}(1).$$

This is because

$$\begin{aligned} Lq &= L \sum_{i=N_p+1}^{\infty} (q, e_i) e_i \\ &= \epsilon A \sum_{i=N_p+1}^{\infty} (q, e_i) e_i \\ &= \frac{1}{\lambda_{N_p+1}} \sum_{i=N_p+1}^{\infty} \lambda_i (q, e_i) e_i \\ &= \sum_{i=N_p+1}^{\infty} \tilde{\lambda}_i (q, e_i) e_i, \quad \tilde{\lambda}_i = \lambda_i / \lambda_{N_p+1} \geq 1 \end{aligned}$$

and

$$|Lq| = \left| \sum_{i=N_p+1}^{\infty} \tilde{\lambda}_i (q, e_i) e_i \right| \geq \left| \sum_{i=N_p+1}^{\infty} (q, e_i) e_i \right| = |q|.$$

Multiplying equation (1.3) by ϵ we obtain a perturbed equation

$$\epsilon \dot{q} + Lq + \epsilon QF(p + q) = 0, \quad (2.1)$$

where operators L and Q are linear and the overdot denotes a derivative with respect to the independent variable t .

Here, we apply the perturbation technique for the perturbed equation (2.1) for q . This perturbed equation (2.1) is a regular perturbation problem because its solution, say $q(x, t, \epsilon)$, converges as $\epsilon \rightarrow 0$, (i.e., $N_p \rightarrow \infty$ uniformly with respect to the independent variables x and t) to the zero function which is the solution of the limiting problem $Lq = 0$.

So the idea is to expand the solution $q(x, t, \epsilon)$ in a power series in ϵ ,

$$q(x, t, \epsilon) = \phi_0(x, t) + \epsilon \phi_1(x, t) + \epsilon^2 \phi_2(x, t) + \dots \quad (2.2)$$

and use a partial sum of the infinite series (2.2) as an approximation of the exact $q(x, t, \epsilon)$

$$q_k(t) = \sum_{i=0}^k \epsilon^i \phi_i(t) \quad (2.3)$$

where the spatial index is suppressed to simplify the notation. (Hereafter we suppress the spatial index, i.e., $q_k(t) = q_k(x, t)$ and $\phi_i(t) = \phi_i(x, t)$.) And the unknown functions $\phi_i(t)$ are solved recursively, i.e., in the order $\phi_0, \phi_1, \dots, \phi_k$.

By substituting the finite series expansion (2.3) into our perturbed equation (2.1) and doing a derivative with respect to t we obtain

$$\begin{aligned} \epsilon[\dot{\phi}_0 + \epsilon\dot{\phi}_1 + \dots + \epsilon^k\dot{\phi}_k] + L(\phi_0 + \epsilon\phi_1 + \dots + \epsilon^k\phi_k) \\ + \epsilon QF(p + \phi_0 + \epsilon\phi_1 + \dots + \epsilon^k\phi_k) = 0, \end{aligned} \quad (2.4)$$

where ϕ_i 's are functions of x and t .

Collecting coefficients of equal powers of ϵ in equation (2.4) gives

$$L\phi_0 + \epsilon[\dot{\phi}_0 + L\phi_1 + QF(p + \phi_0)] + \dots = 0, \quad (2.5)$$

where only terms up to $\mathcal{O}(\epsilon)$ have been retained. Here, we assume that $QF(p + \phi_0)$ is constant order with respect to ϵ , i.e.,

$$QF(p + \phi_0) = \mathcal{O}(1). \quad (2.6)$$

Equating the coefficient of ϵ^0 to zero in (2.5) yields

$$\begin{aligned} \phi_0 &= 0, \\ \dot{\phi}_0 &= 0. \end{aligned}$$

And equating the coefficient of ϵ^1 to zero in (2.5), we obtain

$$L\phi_1 + QF(p) = 0,$$

i.e.,

$$\phi_1 = -L^{-1}QF(p). \quad (2.7)$$

Moreover, our assumption (2.6) can be rewritten as

$$QF(p) = \mathcal{O}(1). \quad (2.8)$$

To obtain the higher-order terms up to $\mathcal{O}(\epsilon^k)$ in the power series solution (2.3), the nonlinear term F satisfies the condition for Taylor's theorem to use Taylor's formula for $QF\left(p + \sum_{i=1}^k \epsilon^i \phi_i\right)$ about p . If $F : R \rightarrow R$ be of class \mathcal{C}^k , we can consider Taylor's

formula for $F\left(p + \sum_{i=1}^k \epsilon^i \phi_i\right)$:

$$\begin{aligned}
& F\left(p + \sum_{i=1}^k \epsilon^i \phi_i\right) \\
&= F(p) + F'(p) \left[\sum_{i=1}^k \epsilon^i \phi_i \right] + \cdots + \frac{1}{j!} F^{(j)}(p) \left[\sum_{i=1}^k \epsilon^i \phi_i \right]^j \\
&+ \cdots + \frac{1}{k!} F^{(k)}(\tilde{p}) \left[\sum_{i=1}^k \epsilon^i \phi_i \right]^k, \tag{2.9}
\end{aligned}$$

where the prime denotes the derivative with respect to p and the value of \tilde{p} lies between p and $p + \sum_{i=1}^k \epsilon^i \phi_i$.

We now expand (2.9) in the form of a power series in ϵ . Since we are only interested in terms up to $\mathcal{O}(\epsilon^k)$, we only keep terms up to $\mathcal{O}(\epsilon^k)$ inside the square brackets in (2.9), that is,

$$\left[\sum_{i=1}^k \epsilon^i \phi_i \right]^j = \left[\sum_{i=1}^{k-j+1} \epsilon^i \phi_i \right]^j + \mathcal{O}(\epsilon^{k+1}), \quad \text{for } j = 1, 2, \dots, k. \tag{2.10}$$

Thus by using the relationship (2.10) we can rewrite Taylor's formula (2.9) in the form of power series in ϵ as follows:

$$\begin{aligned}
& F\left(p + \sum_{i=1}^k \epsilon^i \phi_i\right) \\
&= F(p) + F'(p) \left[\sum_{i=1}^k \epsilon^i \phi_i \right] + \cdots + \frac{1}{j!} F^{(j)}(p) \left[\sum_{i=1}^{k-j+1} \epsilon^i \phi_i \right]^j \\
&+ \cdots + \frac{1}{k!} F^{(k)}(\tilde{p}) \left[\epsilon \phi_1 \right]^k + \mathcal{O}(\epsilon^{k+1}) \\
&:= F_0 + \epsilon F_1 + \cdots + \epsilon^j F_j + \cdots + \epsilon^k F_k + \mathcal{O}(\epsilon^{k+1}), \tag{2.11}
\end{aligned}$$

$$\begin{aligned}
F_0 &= F(p), \quad \text{for } j = 1, 2, \dots, k-1, \\
F_j &= F'(p) \phi_j + \frac{1}{2!} F''(p) \left[\sum_{i_1+i_2=j} \phi_{i_1} \phi_{i_2} \right] + \frac{1}{3!} F^{(3)}(p) \left[\sum_{i_1+i_2+i_3=j} \phi_{i_1} \phi_{i_2} \phi_{i_3} \right] \\
&+ \cdots + \frac{1}{j!} F^{(j)}(p) \left[\sum_{i_1+i_2+\dots+i_j=j} \phi_{i_1} \phi_{i_2} \cdots \phi_{i_j} \right], \tag{2.12}
\end{aligned}$$

for $0 < i_1, i_2, \dots, i_j < j < k$, and

$$F_k = F'(p)\phi_k + \frac{1}{2!}F''(p) \left[\sum_{i_1+i_2=k} \phi_{i_1}\phi_{i_2} \right] + \frac{1}{3!}F^{(3)}(p) \left[\sum_{i_1+i_2+i_3=k} \phi_{i_1}\phi_{i_2}\phi_{i_3} \right] \\ + \dots + \frac{1}{k!}F^{(k)}(\tilde{p})\phi_1^k$$

where the value of \tilde{p} lies between p and $p + \sum_{i=1}^k \epsilon^i \phi_i$.

For instance, the first three terms F_1 , F_2 and F_3 are

$$F_1 = F'(p)\phi_1, \\ F_2 = F'(p)\phi_2 + \frac{1}{2!}F''(p) \left[\sum_{i_1+i_2=2} \phi_{i_1}\phi_{i_2} \right] \\ = F'(p)\phi_2 + \frac{1}{2!}F''(p) [\phi_1\phi_1] \\ = F'(p)\phi_2 + \frac{1}{2!}F''(p)\phi_1^2, \\ F_3 = F'(p)\phi_3 + \frac{1}{2!}F''(p) \left[\sum_{i_1+i_2=3} \phi_{i_1}\phi_{i_2} \right] + \frac{1}{3!}F^{(3)}(p) \left[\sum_{i_1+i_2+i_3=3} \phi_{i_1}\phi_{i_2}\phi_{i_3} \right] \\ = F'(p)\phi_3 + \frac{1}{2!}F''(p) [\phi_1\phi_2 + \phi_2\phi_1] + \frac{1}{3!}F^{(3)}(p) [\phi_1\phi_1\phi_1] \\ = F'(p)\phi_3 + F''(p)\phi_1\phi_2 + \frac{1}{3!}F^{(3)}(p)\phi_1^3.$$

Since the operator Q is linear, Taylor's formula for F defined by (2.11) can be used directly to induce a Taylor expansion for $QF(p + \epsilon\phi_1 + \dots + \epsilon^k\phi_k)$ about p :

$$QF \left(p + \sum_{i=1}^k \epsilon^i \phi_i \right) = QF_0 + \epsilon QF_1 + \epsilon^2 QF_2 + \dots + \epsilon^k QF_k + \mathcal{O}(\epsilon^{k+1}). \quad (2.13)$$

Using (2.13), we can rewrite equation (2.4) as

$$\left[\epsilon^2 \dot{\phi}_1 + \epsilon^3 \dot{\phi}_2 + \dots + \epsilon^k \dot{\phi}_{k-1} \right] + \left[\epsilon L\phi_1 + \epsilon^2 L\phi_2 + \dots + \epsilon^k L\phi_k \right] \\ + \left[\epsilon QF_0 + \epsilon^2 QF_1 + \dots + \epsilon^k QF_{k-1} \right] = 0. \quad (2.14)$$

Only if each QF_i , $i = 0, 1, 2, \dots, k$, is constant order with respect to ϵ , i.e.,

$$QF_i = \mathcal{O}(1) \quad i = 0, 1, 2, \dots, k-1, \quad (2.15)$$

collecting coefficients of equal powers of ϵ in equation (2.14) gives

$$\epsilon \left[L\phi_1 + QF_0 \right] + \epsilon^2 \left[\dot{\phi}_1 + L\phi_2 + QF_1 \right] + \cdots + \epsilon^k \left[\dot{\phi}_{k-1} + L\phi_k + QF_{k-1} \right] = 0,$$

where terms up to $\mathcal{O}(\epsilon^k)$ have been retained.

Equating the coefficient of each power of ϵ to zero, we obtain the explicit formula for each ϕ_i as follows:

$$\begin{aligned} \phi_1 &= -L^{-1}QF_0 = -L^{-1}QF(p), \\ \phi_2 &= -L^{-1}(QF_1 + \dot{\phi}_1) = -L^{-1} \left(QF'(p)\phi_1 + \dot{\phi}_1 \right), \\ \phi_3 &= -L^{-1}(QF_2 + \dot{\phi}_2) = -L^{-1} \left(QF'(p)\phi_2 + \frac{1}{2!}QF''(p)\phi_1^2 + \dot{\phi}_2 \right), \\ &\vdots \\ \phi_k &= -L^{-1}(QF_{k-1} + \dot{\phi}_{k-1}) \\ &= -L^{-1} \left(QF'(p)\phi_{k-1} + \frac{1}{2!}QF''(p) \sum_{i_1+i_2=k-1} [\phi_{i_1}\phi_{i_2}] + \right. \\ &\quad \left. \frac{1}{3!}QF^{(3)}(p) \sum_{i_1+i_2+i_3=k-1} [\phi_{i_1}\phi_{i_2}\phi_{i_3}] + \cdots + \frac{1}{(k-1)!}QF^{(k-1)}(p)\phi_1^{k-1} + \dot{\phi}_{k-1} \right). \end{aligned}$$

Thus we can get approximate solutions $q_k(t)$'s as finite sums of $\phi_i(t)$'s

$$q_k(t) = \sum_{i=1}^k \epsilon^i \phi_i(t), \quad k = 1, 2, \dots. \quad (2.16)$$

Our approximate inertial manifolds \mathcal{M}_k are closely related to these approximations, q_k .

2.2. Construction of approximate inertial manifolds

The aim of this subsection is to present the construction of the sequence $(\mathcal{M}_k)_{k \in \mathbb{Z}_+}$ of approximate inertial manifolds in detail. That is, the approximate inertial manifolds \mathcal{M}_k are constructed as the graphs of the functions $\Phi_k : PD(A) \rightarrow QD(A)$ which will be suitable approximations of the previous perturbation results under the assumption that the nonlinear operator F has the Taylor expansion given by (2.9).

Considering $k = 1$ in equation (2.16) gives the first manifold \mathcal{M}_1 when F is a differentiable function satisfying the condition (2.15). In practice, we assume that F is a C^1 function which satisfies

$$F(p) = \mathcal{O}(1) \quad \text{with} \quad |F'| \leq K_{11} \quad (2.17)$$

where the positive constant K_{11} is constant order with respect to ϵ .

The approximate solution of $q(x, t)$ in (1.3), say $q_1(t)$, is

$$q_1(t) = \epsilon\phi_1(t) = -\epsilon L^{-1}QF(p(t)) = -A^{-1}QF(p(t)). \quad (2.18)$$

Since q_1 is a function of t through $p(t)$, the related function Φ_1 , the function of p , can be defined by q_1 itself, i.e.,

$$\Phi_1(p) = -A^{-1}QF(p). \quad (2.19)$$

The graph of the function Φ_1 is the approximate inertial manifold defined in C. Foias, O. Manley and R. Temam [6] in the context of the Navier-Stokes equation and subsequently used in many other articles, both theoretical and numerical. (see [5], [9], [11])

Next we construct another manifold \mathcal{M}_2 if the nonlinear operator F is a C^2 function which satisfies the sufficient conditions of (2.15):

$$F(p) = \mathcal{O}(1), \quad \text{with} \quad |F'| \leq K_{21} \quad \text{and} \quad |F''| \leq K_{22}, \quad (2.20)$$

where positive constants K_{21} and K_{22} are constant order with respect to ϵ .

In (2.16), $q_2(t)$ is rewritten as follows:

$$\begin{aligned} q_2(t) &= \epsilon\phi_1(t) + \epsilon^2\phi_2(t) \\ &= -\epsilon L^{-1} \left(QF(p(t)) + QF'(p(t))\epsilon\phi_1(t) + \epsilon\dot{\phi}_1(t) \right) \\ &= -A^{-1} \left(QF(p(t)) + QF'(p(t))q_1(t) + \dot{q}_1(t) \right) \end{aligned} \quad (2.21)$$

where the overdot and the prime denote the derivative with respect to time and p , respectively.

Here, at the second step $k = 2$, we will update \dot{q}_1 in (2.21) using Φ_1 , the best approximation of q that we have so far obtained. That is, the nonlinear term $F(p)$ in (2.19) is replaced by $F(p + \Phi_1(p))$. And we can rewrite $\dot{q}_1(t)$ as follows:

$$\begin{aligned} \dot{q}_1(t) &= -\frac{\partial}{\partial t} A^{-1}QF(p + \Phi_1(p)) \\ &= -A^{-1}QF'(p + \Phi_1(p))(\dot{p} + \dot{\Phi}_1(p)) \end{aligned} \quad (2.22)$$

where the second equality (2.22) comes from the chain rule and the overdot denotes the derivative with respect to time.

In (2.22) $\dot{p} + \dot{\Phi}_1(p)$ can be approximated by \dot{p} , and \dot{p} is better approximated using equation (1.2) by

$$\dot{p} = -Ap - PF(p + \Phi_1(p)).$$

Hence, we can derive a better value for \dot{q}_1 in (2.21) and denote it by $\dot{\Phi}_1$

$$\dot{\Phi}_1(p) = A^{-1}QF'(p + \Phi_1(p)) \left(Ap + PF(p + \Phi_1(p)) \right). \quad (2.23)$$

Thus the function Φ_2 is defined by

$$\Phi_2(p) = -A^{-1} \left(QF(p) + QF'(p)\Phi_1(p) + \dot{\Phi}_1(p) \right), \quad (2.24)$$

where $\dot{\Phi}_1$ is given by (2.23).

Now we aim to generalize this idea to construct \mathcal{M}_k , ($k \geq 3$), recursively under the assumption that the nonlinear operator F is a C^k function which satisfies the corresponding sufficient conditions of (2.15).

We start by rewriting q_k in (2.16)

$$\begin{aligned} q_k &= \epsilon\phi_1 + \epsilon^2\phi_2 + \cdots + \epsilon^k\phi_k \\ &= -\epsilon L^{-1} \left(QF_0 + \epsilon QF_1 + \epsilon^2 QF_2 + \cdots + \epsilon^{k-1} QF_{k-1} + \epsilon^1 \dot{\phi}_1 + \epsilon^2 \dot{\phi}_2 + \cdots + \epsilon^{k-1} \dot{\phi}_{k-1} \right) \\ &= -A^{-1} \left(QF(p) + QF'(p) \left[\sum_{i=1}^{k-1} \epsilon^i \phi_i \right] + \frac{1}{2!} QF''(p) \left[\sum_{i=1}^{k-2} \epsilon^i \phi_i \right]^2 + \cdots \right. \\ &\quad \left. + \frac{1}{(k-1)!} QF^{(k-1)}(p) \left[\epsilon\phi_1 \right]^{k-1} + \dot{q}_{k-1} \right) + \mathcal{O}(\epsilon^{k+1}) \\ &= -A^{-1} \left(QF(p) + QF'(p)q_{k-1} + \frac{1}{2!} QF''(p)q_{k-2}^2 + \cdots \right. \\ &\quad \left. + \frac{1}{(k-1)!} QF^{(k-1)}(p)q_1^{k-1} + \dot{q}_{k-1} \right) + \mathcal{O}(\epsilon^{k+1}). \end{aligned} \quad (2.25)$$

We need to obtain better approximation for \dot{q}_{k-1} by using the known best approximation Φ_{k-1} of q up to this stage. That is, we define $\dot{\Phi}_{k-1}$ by

$$\dot{\Phi}_{k-1}(p) = A^{-1} QF'(p + \Phi_{k-1}(p)) \left(Ap + PF(p + \Phi_{k-1}(p)) \right). \quad (2.26)$$

Thus we can construct the manifold \mathcal{M}_k with the equation

$$q = \Phi_k(p), \quad \Phi_k : PD(A) \rightarrow QD(A).$$

Here, $\Phi_k(p)$ can be defined recursively as

$$\begin{aligned} &\Phi_k(p) \\ &= -A^{-1} \left(QF(p) + QF'(p)\Phi_{k-1} + \frac{1}{2!} QF''(p)\Phi_{k-2}^2 + \cdots + \right. \\ &\quad \left. \frac{1}{(k-1)!} QF^{(k-1)}(p)\Phi_1^{k-1} + \dot{\Phi}_{k-1} \right), \end{aligned} \quad (2.27)$$

where $\dot{\Phi}_{k-1}(p)$ is defined in (2.26).

3. Numerical experiments

In this section we present some numerical experiments to support the results of the previous section. We will show that the higher order approximate inertial manifold $\Phi_2(p)$ gives more accurate results than $\Phi_1(p)$ and the Euler-Galerkin method. We investigate two numerical examples of the reaction diffusion equation subject to homogeneous Dirichlet boundary conditions with different nonlinear terms: 1. non-polynomial nonlinearity and 2. polynomial nonlinearity.

For the purpose of computational demonstrations, we consider the reaction diffusion equation

$$u_t - \nu u_{xx} + F(u) = 0, \quad x \in (0, \pi), \quad t > 0 \quad (3.1)$$

subject to homogeneous Dirichlet boundary conditions,

$$u(0, t) = u(\pi, t) = 0, \quad t \geq 0 \quad (3.2)$$

where the diffusivity ν is a positive constant. The function $F(u)$ is nonlinear. We note that the 1-D Laplacian operator $-\partial_{xx}$ with the Dirichlet boundary condition (3.2) is a linear, unbounded, self-adjoint and positive operator possessing a compact inverse.

We apply semi-finite difference method to obtain a system of ordinary differential equations. A continuous function $u = u(x, t)$ is discretized on an equidistant spatial grid $x_j = jh$, $1 \leq j \leq M$, where $h = \frac{\pi}{M+1}$ is the step size in spatial direction. Discretizing the boundary valued problem (3.1), (3.2) in the spatial variable it can be reduced to a system of ordinary differential equations: for $j = 1, 2, \dots, M$

$$\begin{aligned} \frac{du_j}{dt} - \frac{\nu}{h^2} (u_{j+1} - 2u_j + u_{j-1}) + F(u_j) &= 0 \\ u_0 = u_{M+1} &= 0 \end{aligned} \quad (3.3)$$

where M is the number of unknowns and indices 0 and $M+1$ denote the boundary values.

Let us consider a column vector u :

$$u(t) = (u_1, \dots, u_M)^T$$

whose components are real valued functions of t . In matrix form the ODE system (3.3) can be written as

$$\frac{du}{dt} + Au + F(u) = 0, \quad (3.4)$$

where A is a tridiagonal matrix of order M :

$$A = \text{tridiag} \left(-\frac{\nu}{h^2}, 2\frac{\nu}{h^2}, -\frac{\nu}{h^2} \right),$$

and $F(u)$ is a column vector of the length M with the contribution from the homogeneous boundary condition (3.2) :

$$F(u) = \begin{pmatrix} F(u_1) - \frac{\nu}{h^2}u_0 \\ F(u_2) \\ \vdots \\ F(u_{M-1}) \\ F(u_M) - \frac{\nu}{h^2}u_{M+1} \end{pmatrix} = \begin{pmatrix} F(u_1) \\ \vdots \\ F(u_M) \end{pmatrix} \quad (3.5)$$

This ODE system (3.4) can be solved using spectral methods by projecting the set of equations in (3.4) onto the eigenbasis of A (see [1]). Let E be the matrices whose columns are the eigenvectors of A , ordered in terms of increasing eigenvalues $0 < \lambda_1 \leq \lambda_2 \leq \dots \leq \lambda_M$.

Let $U = E^T u$, i.e., $u = EU$. Substituting EU into u and multiplying (3.4) by E^T , we obtain

$$\frac{dU}{dt} + \Lambda U + G(U) = 0, \quad (3.6)$$

where

$$\begin{aligned} \Lambda &= E^T A E \\ &= \text{diag}(\lambda_1, \lambda_2, \dots, \lambda_M) \\ G(U) &= E^T F(EU) \\ &:= (G_1, G_2, \dots, G_M)^T. \end{aligned}$$

Equation (3.6) is the starting point for the computational analysis of approximate inertial manifolds since it is suitable for decomposition into dominant and enslaved modes. We assume that the dominant p -modes are N_p . Then we can decompose equation (3.6) into dominant and enslaved modes, i.e.,

$$\frac{dp}{dt} + \Lambda_p p + G_p(p, q) = 0 \quad (3.7)$$

$$\frac{dq}{dt} + \Lambda_q q + G_q(p, q) = 0 \quad (3.8)$$

where

$$\begin{aligned} \Lambda_p &= \text{diag}(\lambda_1, \lambda_2, \dots, \lambda_{N_p}), \\ \Lambda_q &= \text{diag}(\lambda_{N_p+1}, \lambda_{N_p+2}, \dots, \lambda_M), \\ G_p &= (G_1, G_2, \dots, G_{N_p})^T, \\ G_q &= (G_{N_p+1}, G_{N_p+2}, \dots, G_M)^T, \\ p &= (U_1, U_2, \dots, U_{N_p})^T := (p_1, p_2, \dots, p_{N_p})^T, \\ q &= (U_{N_p+1}, U_{N_p+2}, \dots, U_M)^T := (q_1, q_2, \dots, q_{N_q})^T, \\ (p, q) &= (U_1, U_2, \dots, U_M)^T = (p_1, \dots, p_{N_p}, q_1, \dots, q_{N_q})^T. \end{aligned}$$

The construction of the approximate inertial manifold through the result of the previous section can be given by

$$\Phi_1(p) = -\Lambda_q^{-1}G_q(p) \quad (3.9)$$

$$\Phi_2(p) = -\Lambda_q^{-1}\left(G_q(p) + G'_q(p)\Phi_1(p) + \dot{\Phi}_1(p)\right) \quad (3.10)$$

$$\dot{\Phi}_1(p) = \Lambda_q^{-1}\left(G'_q(p, \Phi_1(p))(\Lambda_p p + G_p(p, \Phi_1(p)))\right) \quad (3.11)$$

where the overdot and the prime denote the derivative with respect to time and p , respectively.

The approximate inertial manifold (3.9), $q = \Phi_1(p)$, is nothing but FMT AIM in (1.6). The Euler-Galerkin AIM in (1.6) (say, $\Phi(p)$) is given by

$$q = \Phi(p) = -\tau(I + \tau\Lambda_q)^{-1}G_q(p) \quad (3.12)$$

where I is the identity matrix and the time scale τ is equal to $1/\lambda_{N_p+1}$ for the sake of simplicity (see [7]). The standard Galerkin approximation of (3.6) using N_p modes is

$$\frac{dp}{dt} + \Lambda_p p + G_p(p) = 0. \quad (3.13)$$

We will now compare the accuracy of different methods for solving equation (3.1) using the solution obtained by the semi-finite difference method with sufficiently fine discretization as our "exact" solution. We consider four different methods:

1. the standard Galerkin approximation (denoted by SG in Tables and Figures),
2. the Euler-Galerkin approximation of equation (3.12) (denoted by EG),
3. the perturbation method with the first term only (3.9) which was introduced by Foias, Manley, and Temam [6] (denoted by P1),
4. the modified perturbation method with two terms (3.10) and (3.11) (denoted by P2).

We shall compare SG, EG and P1 with our AIM obtained by the modified perturbation method using two terms Φ_1 and Φ_2 in (3.10) and (3.11). All our algorithms are implemented in Matlab and the numerical simulations are performed with the ODESUITE stiff stable integrator ODE15s.

We investigate two numerical examples of the reaction diffusion equation subject to homogeneous Dirichlet boundary conditions

Example 1.

$$\begin{aligned} u_t - \frac{1}{3}u_{xx} - e^{u/(1+au)} &= 0 \\ u(x, 0) &= 0, \quad x \in (0, \pi) \\ u(0, t) = u(\pi, t) &= 0, \quad t \geq 0 \end{aligned}$$

where a is a positive constant.

Example 2.

$$\begin{aligned} u_t - 0.16u_{xx} + u^3 - bu &= 0 \\ u(x, 0) &= \sin x, \quad x \in (0, \pi) \\ u(0, t) = u(\pi, t) &= 0, \quad t \geq 0, \end{aligned}$$

where b is a positive constant.

The first five figures (Figures 1 through 5) are related to the numerical results of Example 1, the non-polynomial nonlinearity example. Figures 1 and 2 show convergence diagrams with errors measured at time $T = 1$. Figure 1 is for different values of the parameter a but for fixed number of unknowns $M = 40$. Figure 2 is for different M but fixed $a = 1$. In these figures, we display the L^2 -errors as a function of N_p . The value N_p is represented on the horizontal axis and the corresponding L^2 -error is on the vertical axis. The value of N_p grows by 4 in the range [4,16] which corresponds to 10% through 40% of the total number of modes M . In each of Figures 3 and 4, we show four plots in which the L^2 -errors are compared for different methods as a function of the parameter a for different N_p 's when $M = 40$ and 80, respectively. In both Figures 3 and 4, N_p has the same four different values 4, 8, 12, and 16 which correspond to 10% through 40% of $M = 40$ in Figure 3 and 5% through 20% of $M = 80$ in Figure 4. In each plot, the value of a is represented on the horizontal axis and the corresponding L^2 -error is on the vertical axis. Here, the parameter a grows in powers of 2 in the range $[2^{-4}, 2^4]$. In Figure 5, we show four plots of different nonlinear terms and their first and second derivatives. Each plot has different values of $a = 1/16, 1/2, 2, \text{ and } 16$.

The next six figures (Figures 6 through 11) are related to the numerical results for Example 2, the polynomial nonlinearity example. Specifically, Figures 6 through 10 correspond to Figures 1 through 5, respectively. Here, the L^2 -error is measured at time $T = 40$. The final time $T = 40$ was chosen well into the steady state by demanding that $|u(T) - u(T - 1)| \leq 10^{-11}$. In Figures 8 and 9, the parameter b has four values of 1, 2, 3, and 4. Figure 11 shows the importance of choosing a sufficiently large value of N_p to achieve better accuracy of our perturbation method with two terms (P2). Here, the L^2 -errors for the Euler-Galerkin method (EG) and the perturbation method with two terms (P2) as a function of b for Example 2 when $M = 40$ are presented.

In Figures 1 and 6, for both non-polynomial and polynomial nonlinearity examples, our perturbation method with two terms P2 is superior to the others for all considered values of N_p (10% through 40% of M). We note that changing the parameter a in Example 1 and the parameter b in Example 2 contributes to significant changes in the derivative terms $F'(u)$ or $F''(u)$. This allows us to study their influence on the performance of all algorithms. For all a and b values we considered, P2 is superior to the others when $N_p = 12$ and 16. But for smaller values of $N_p = 4$ and 8, P2 could not improve the accuracy when $a = 1/16$ and 16 for Example 1 and $b = 4$ for Example 2 (see Figures 1 and 6). This is because P2 needs the conditions (2.20) to be satisfied related to the nonlinear term. When $N_p = 4$, i.e., $\epsilon = 1/\lambda_5$, the first or the second

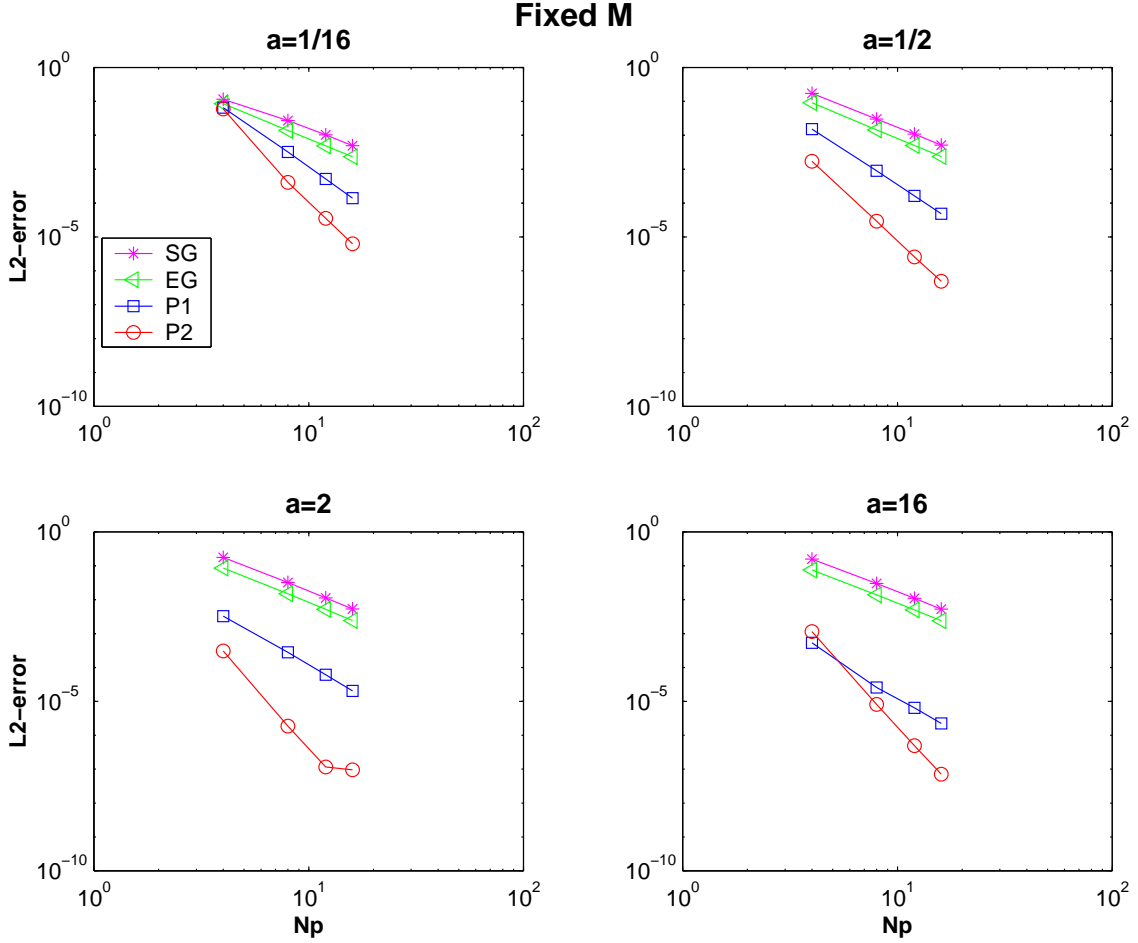


Figure 1: Convergence result of Example 1 for the number of unknowns $M = 40$: The L^2 -errors committed by the four different methods with different value of $N_p = 4, 8, 12, 16$ and the parameter a for the reaction diffusion equation with the non-polynomial nonlinearity.

derivative of the nonlinear term is increasing too much to satisfy the conditions (2.20) as u is increasing (see Figure 5 and 10). This indicates that $N_p = 4$ may be too small to satisfy the conditions (2.20). We conclude that the conditions (2.20) for P2 must be satisfied in order to gain improvement in accuracy.

Furthermore, we can see from Figures 2 and 7 that the accuracy depends on ϵ , i.e., on the value of N_p and not on the percentage of p -mode (i.e., ratio N_p/M). For example, $N_p = 8$ is 40% of $M = 20$, 20% of $M = 40$ and just 10% of $M = 80$. All these cases show very close L^2 -errors in Figures 2 and 7. This is much clearer in Figures 3, 4, 8, and 9. We have the same pattern of accuracy when we preserve the same ϵ for different values $M = 40$ and 80 in both Example 1 and Example 2.

Finally, we will compare our perturbation method P2 with the Euler-Galerkin method

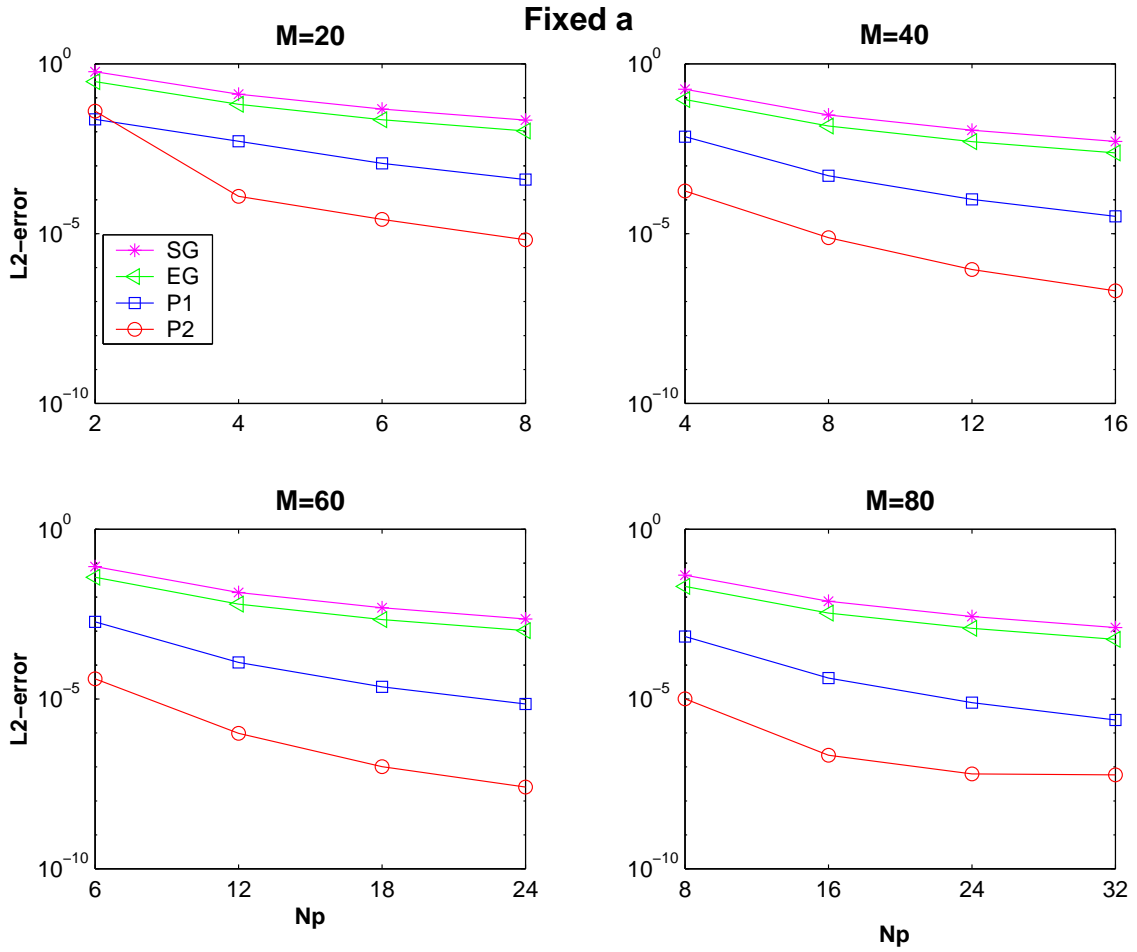


Figure 2: Convergence result of Example 1 for the parameter $a = 1$: The L^2 -errors committed by the four different methods with different N_p and the number of unknowns M . Each N_p is corresponding to 10% through 40% of four different M 's.

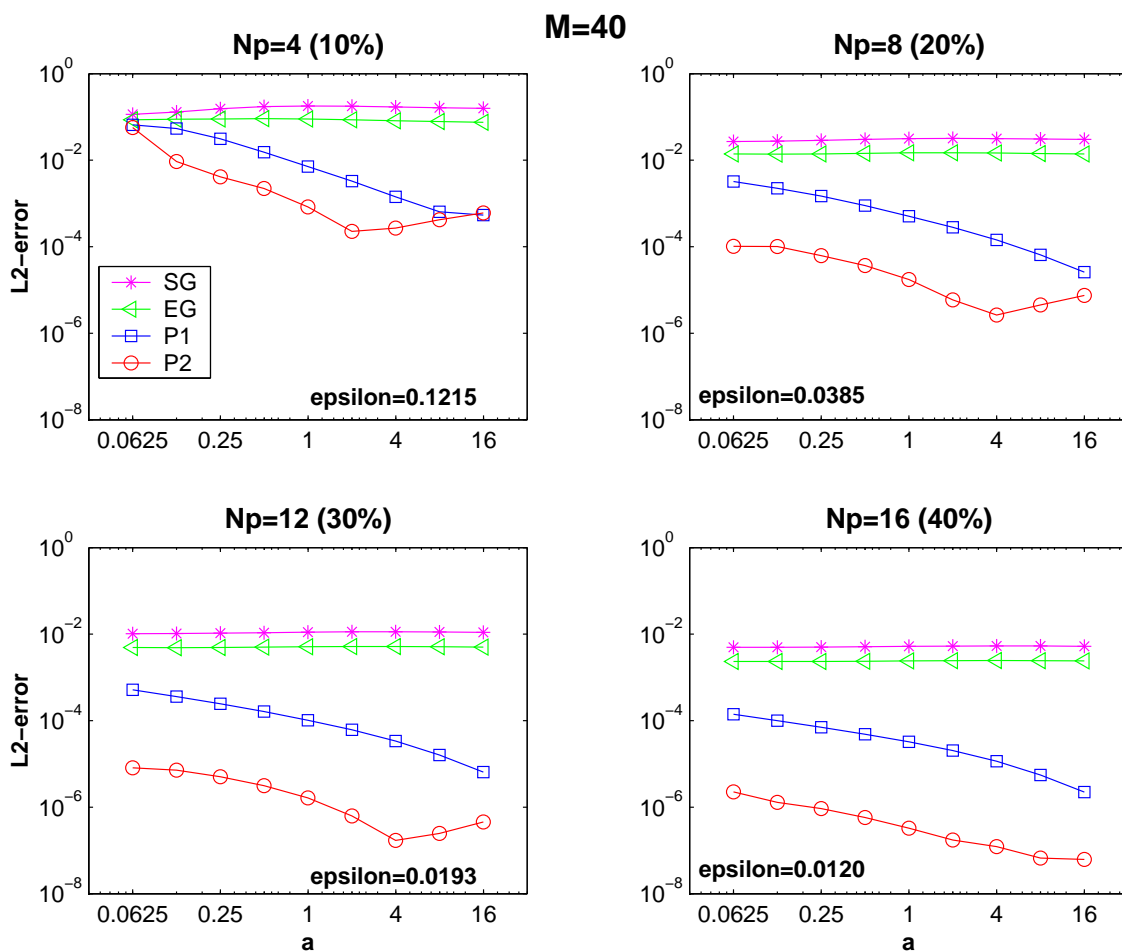


Figure 3: Accuracy of Example 1 as a function of the parameter a for different N_p 's when $M = 40$: The parameter a grows in powers of 2 in the range $[2^{-4}, 2^4]$ for each different value of $N_p = 4, 8, 12, 16$ which is corresponding to 10% through 40% of $M = 40$. Here, epsilon is $\epsilon = 1/\lambda_{N_p+1}$.

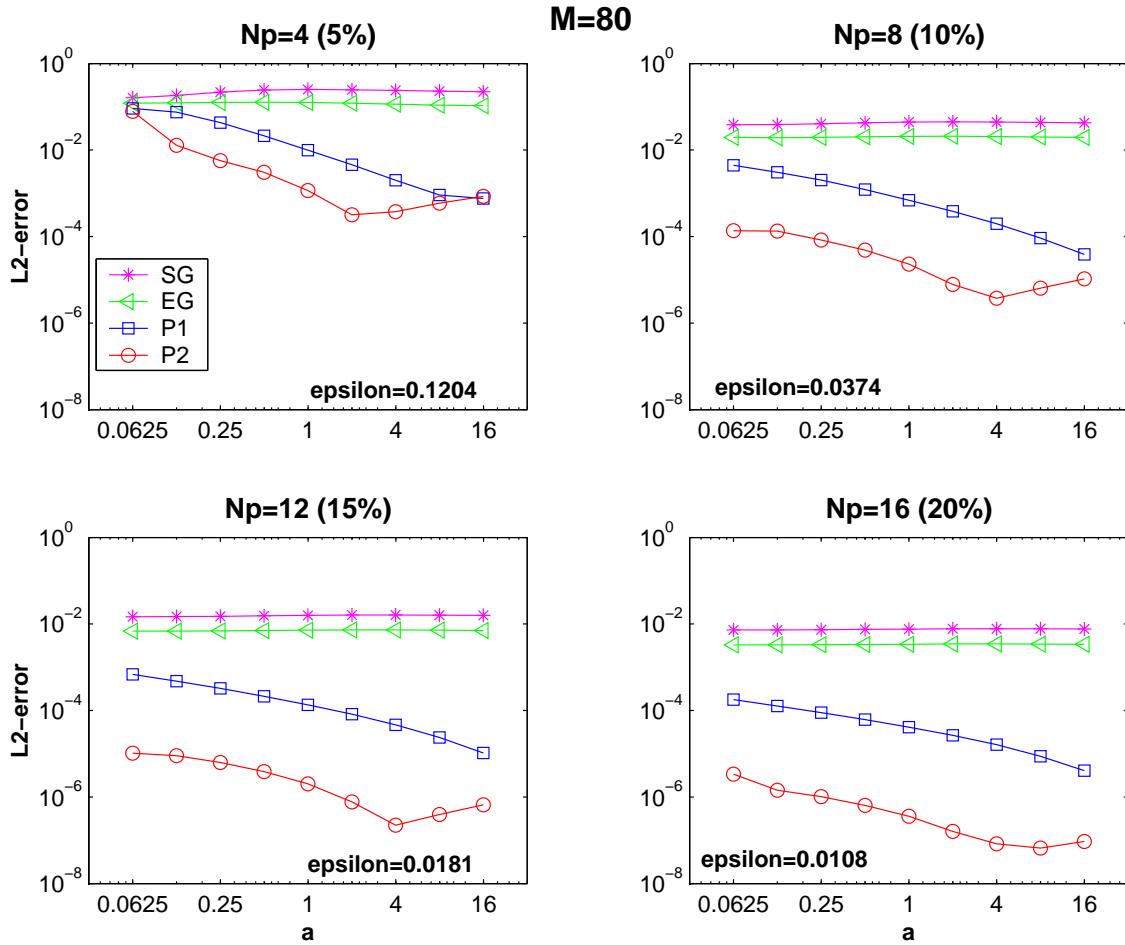


Figure 4: Accuracy of Example 1 as a function of the parameter a for different N_p 's when $M = 80$: The parameter a grows in powers of 2 in the range $[2^{-4}, 2^4]$ for each different value of $N_p = 4, 8, 12, 16$ which is corresponding to 5% through 20% of $M = 80$. Here, epsilon is $\epsilon = 1/\lambda_{N_p+1}$.

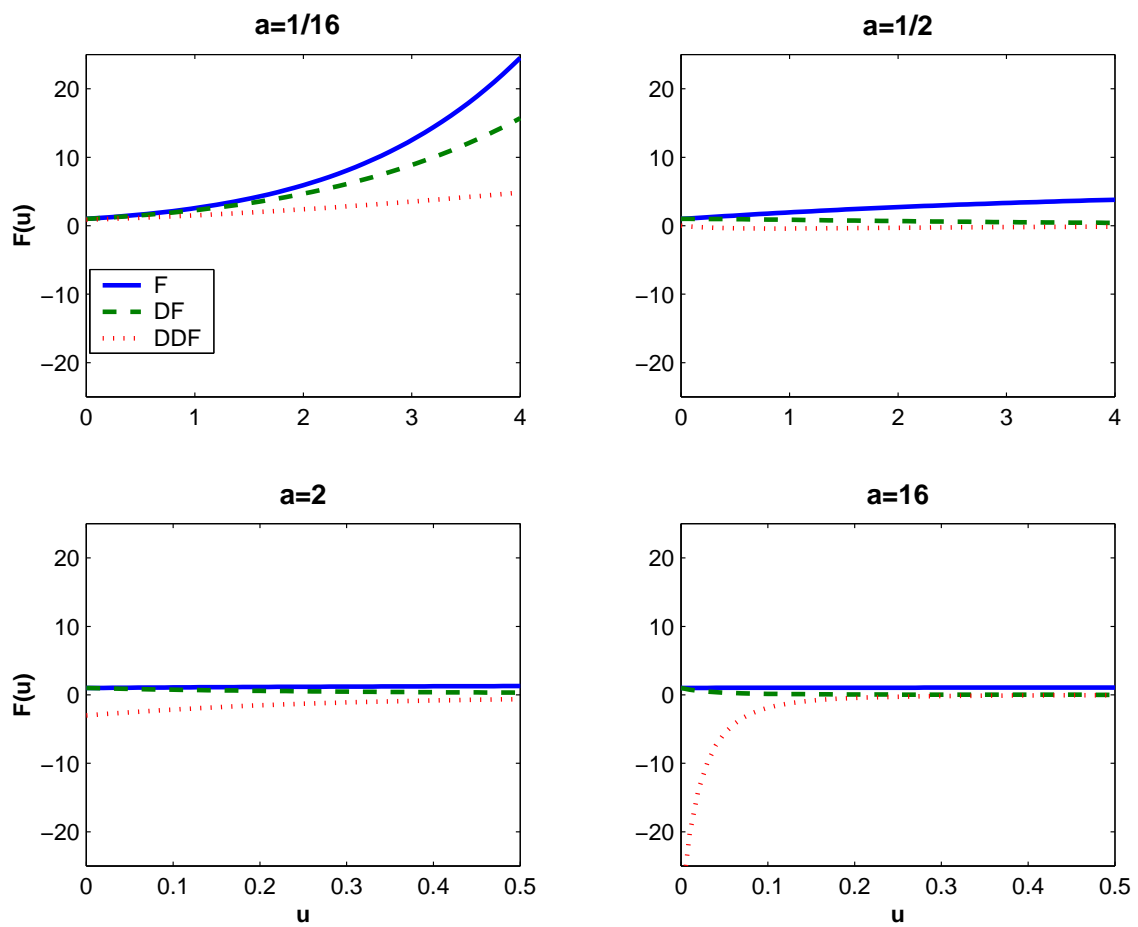


Figure 5: Nonlinear term and its first and second derivatives of Example 1 : $F(u)$ is the nonlinear term of Example 1. F , DF and DDF stand for $F(u)$, $F'(u)$ and $F''(u)$, respectively. This figure helps to see that our AIM P2 needs conditions (2.20).

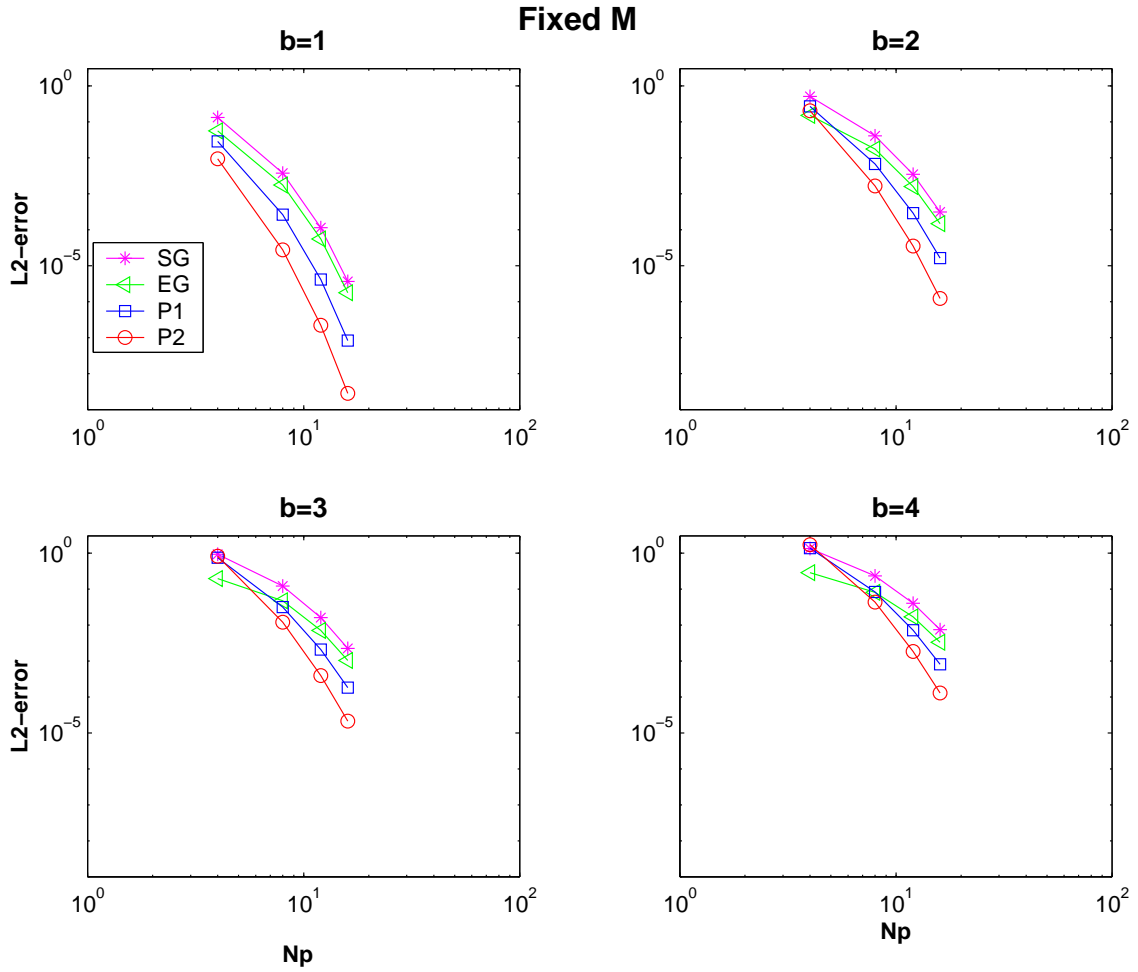


Figure 6: Convergence result of Example 2 for the number of unknowns $M = 40$: The L^2 -errors committed by the four different methods with different value of $N_p = 4, 8, 12, 16$ and the parameter b for the reaction diffusion equation with the polynomial nonlinearity.

EG which has been used in many studies (see [8], [7], [1]). Here, the parameters a and b are fixed to be unity and the total number of modes M is 40 for both examples.

Table 1: Comparison of the accuracy for Example 1 (non-polynomial nonlinearity) when $a = 1$, $M = 40$, and $T = 1$

N_p	ϵ	EG	P2	EG/P2
4	.122	9.00e-2	1.82e-4	495
8	.039	1.48e-2	7.64e-6	1,937
12	.019	5.13e-3	8.85e-7	5,797
16	.012	2.41e-3	2.08e-7	11,587

Table 2: Comparison of the accuracy for Example 2 (polynomial nonlinearity) when $b = 1$ and $M = 40$

N_p	ϵ	T=1			T=40		
		EG	P2	EG/P2	EG	P2	EG/P2
4	.253	2.85e-2	6.31e-3	5	5.59e-2	9.33e-3	6
8	.080	7.71e-4	2.33e-5	33	1.76e-3	2.74e-5	64
12	.040	1.83e-5	2.26e-7	81	5.54e-5	2.21e-7	251
16	.025	4.35e-7	2.54e-8	17	1.79e-6	2.84e-9	630

For the non-polynomial nonlinearity example (Example 1), the error of P2 is at least about 500 times smaller than the error of EG, see Table 1. This Table 1 corresponds to Figure 3. Furthermore, the ratio of error (EG/P2) is increasing up to 10,000 times as N_p is increasing from 4 to 16. However, for the polynomial nonlinearity example (Example 2), P2 could not improve the accuracy as much as for the Example 1. The ratio of error (EG/P2) at $T = 1$ is less than 81, see Table 2. When $T = 40$, the improvement in accuracy by using P2 is substantial for $N_p = 12$ and 16. Thus, we can conclude that P2 gives better accuracy than EG for all reasonable values of $N_p = 4$ through 16. Moreover, its improvement in accuracy increases as N_p increases.

Summarizing the results of our numerical experiments, we see that P2 improves the accuracy of P1 and that P2 is much more accurate than SG and EG for both polynomial and non-polynomial nonlinearity whenever the value of N_p satisfies conditions (2.20). If N_p is too small to satisfy conditions (2.20), we gain little improvement in accuracy by using our perturbation method P2 (see Figure 11).

4. Concluding remarks

In this paper we have presented the construction of a sequence of approximate inertial manifolds (AIMs) by using a perturbation technique. These approximate inertial manifolds are constructed by modification of our perturbation result depending on the smoothness and boundedness of the nonlinear term $F(u)$. The perturbation result is expressed explicitly as a finite sum in ϵ which is an approximate solution of the q -equation.

Compared with other versions of the nonlinear Galerkin methods such as Foias-Manley-Temam AIM (elsewhere P1) Euler-Galerkin AIM (EG), our AIM obtained by the modified perturbation method with two terms (denoted by P2) is far more accurate for both polynomial and non-polynomial nonlinearities whenever the number of p -modes, N_p , satisfies conditions (2.20). With respect to efficiency, however, our P2

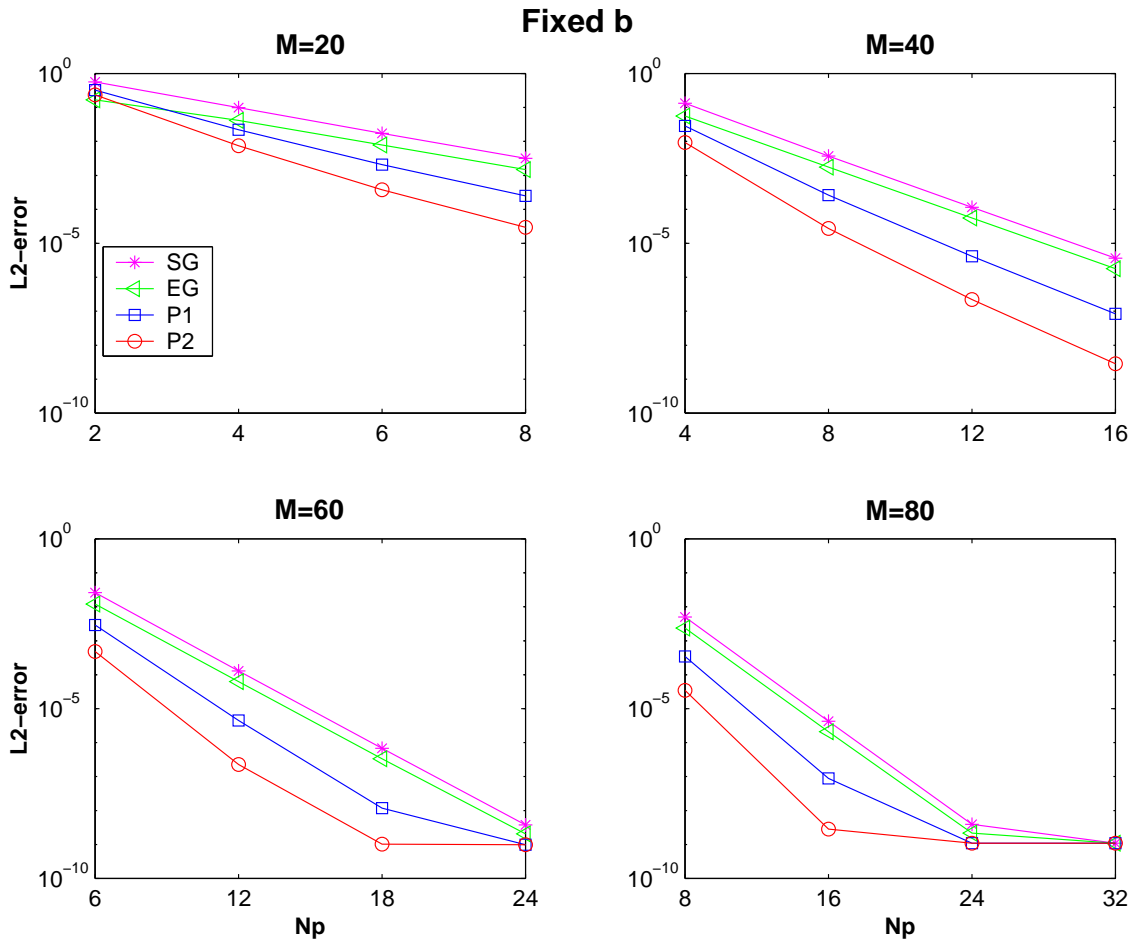


Figure 7: Convergence result of Example 2 for the parameter $b = 1$: The L^2 -errors committed by the four different methods with different N_p and the number of unknowns M . Each N_p is corresponding to 10% through 40% of four different M 's.

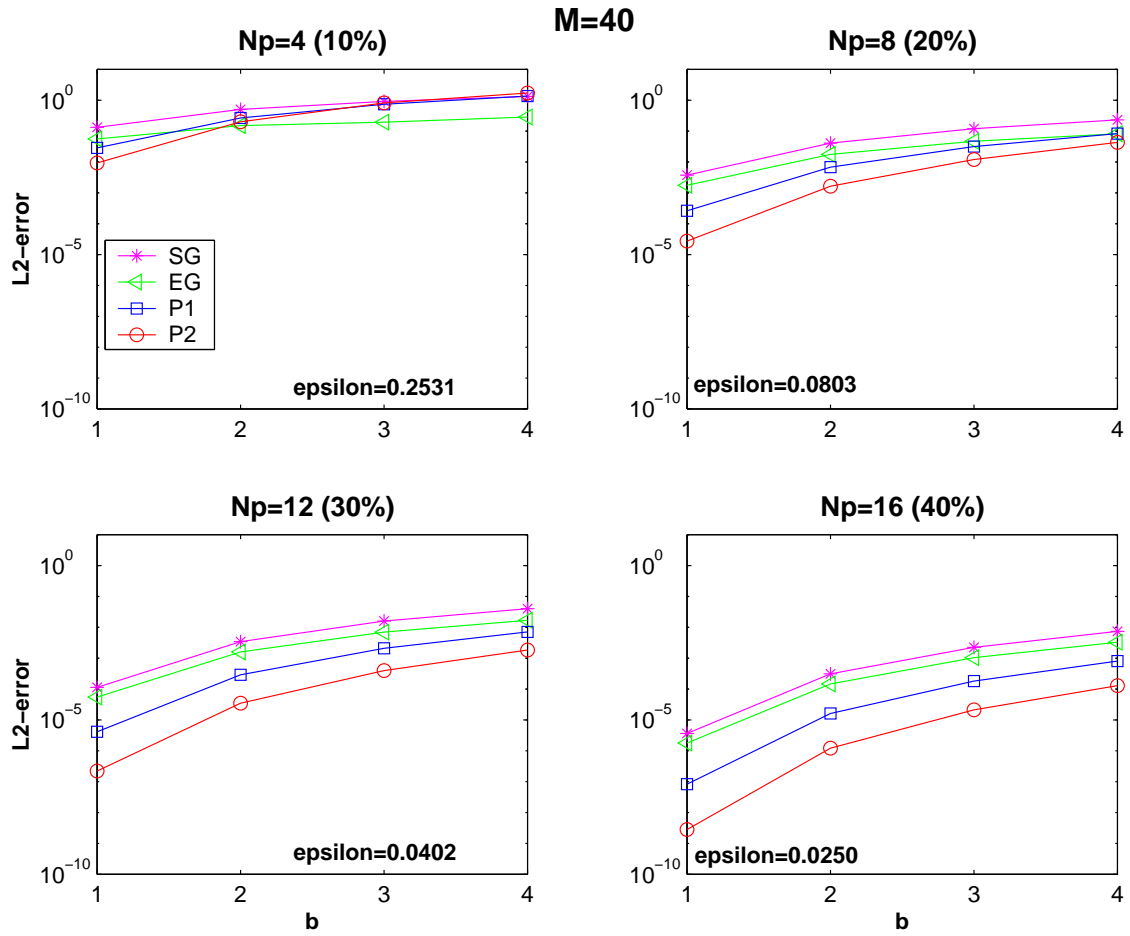


Figure 8: Accuracy of Example 2 as a function of the parameter b for different N_p 's when $M = 40$: The parameter b has four values of 1, 2, 3, and 4 for each different value of $N_p = 4, 8, 12, 16$ which is corresponding to 10% through 40% of $M = 40$. Here, $\epsilon = 1/\lambda_{N_p+1}$.

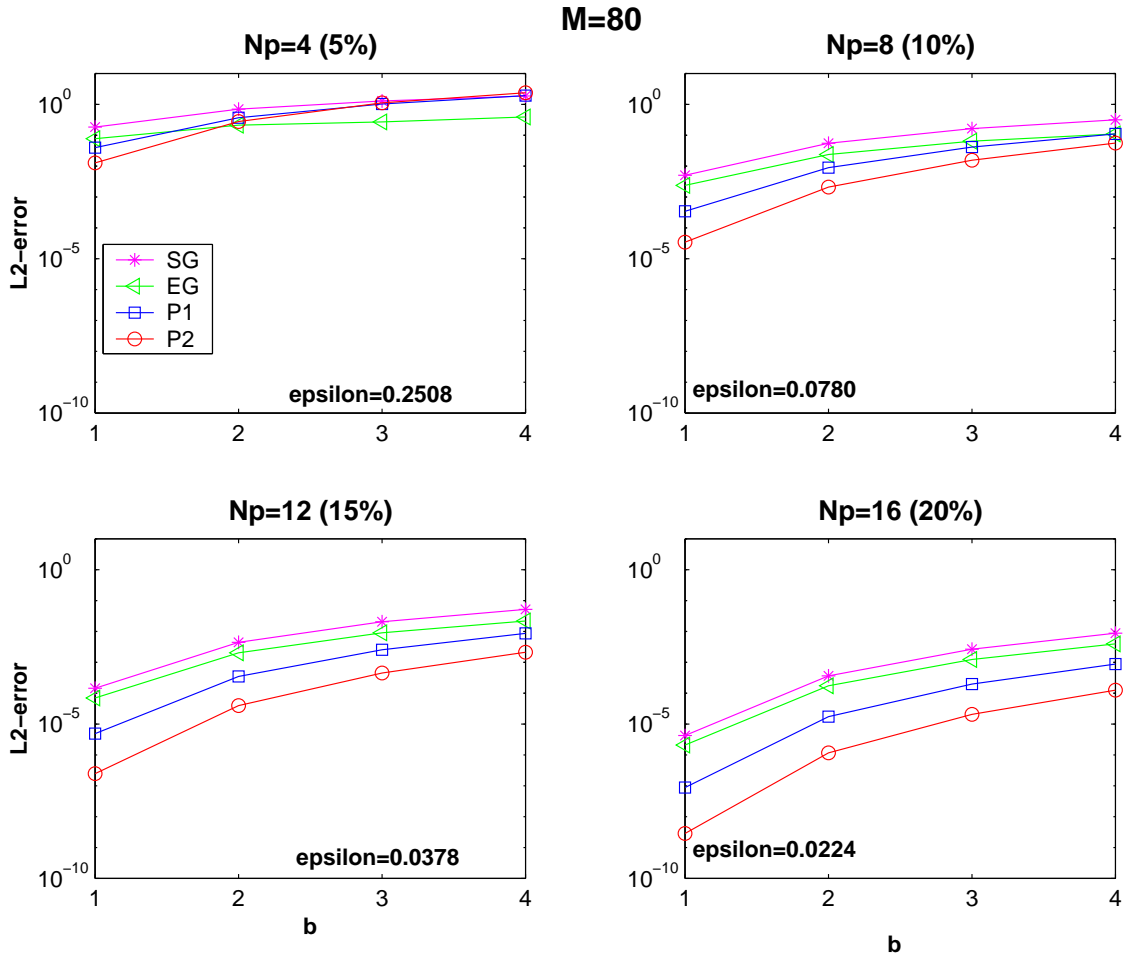


Figure 9: Accuracy of Example 2 as a function of the parameter b for different N_p 's when $M = 80$: The parameter b has four values of 1, 2, 3, and 4 for each different value of $N_p = 4, 8, 12, 16$ which is corresponding to 5% through 20% of $M = 80$. Here, epsilon is $\epsilon = 1/\lambda_{N_p+1}$.

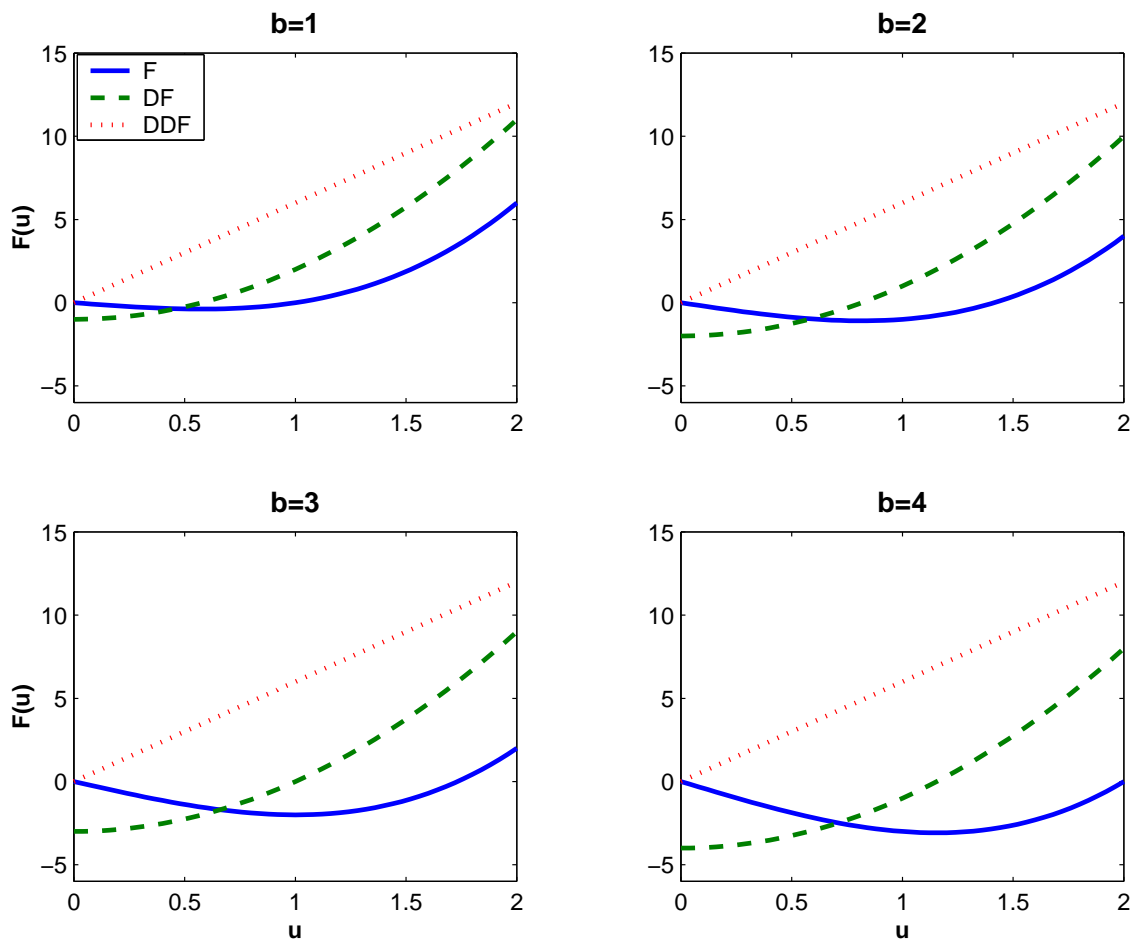


Figure 10: Nonlinear term and its first and second derivatives of Example 2 : $F(u)$ is the nonlinear term of Example 2. F , DF and DDF stand for $F(u)$, $F'(u)$ and $F''(u)$, respectively. This figure helps to see that our AIM P2 needs conditions (2.20).

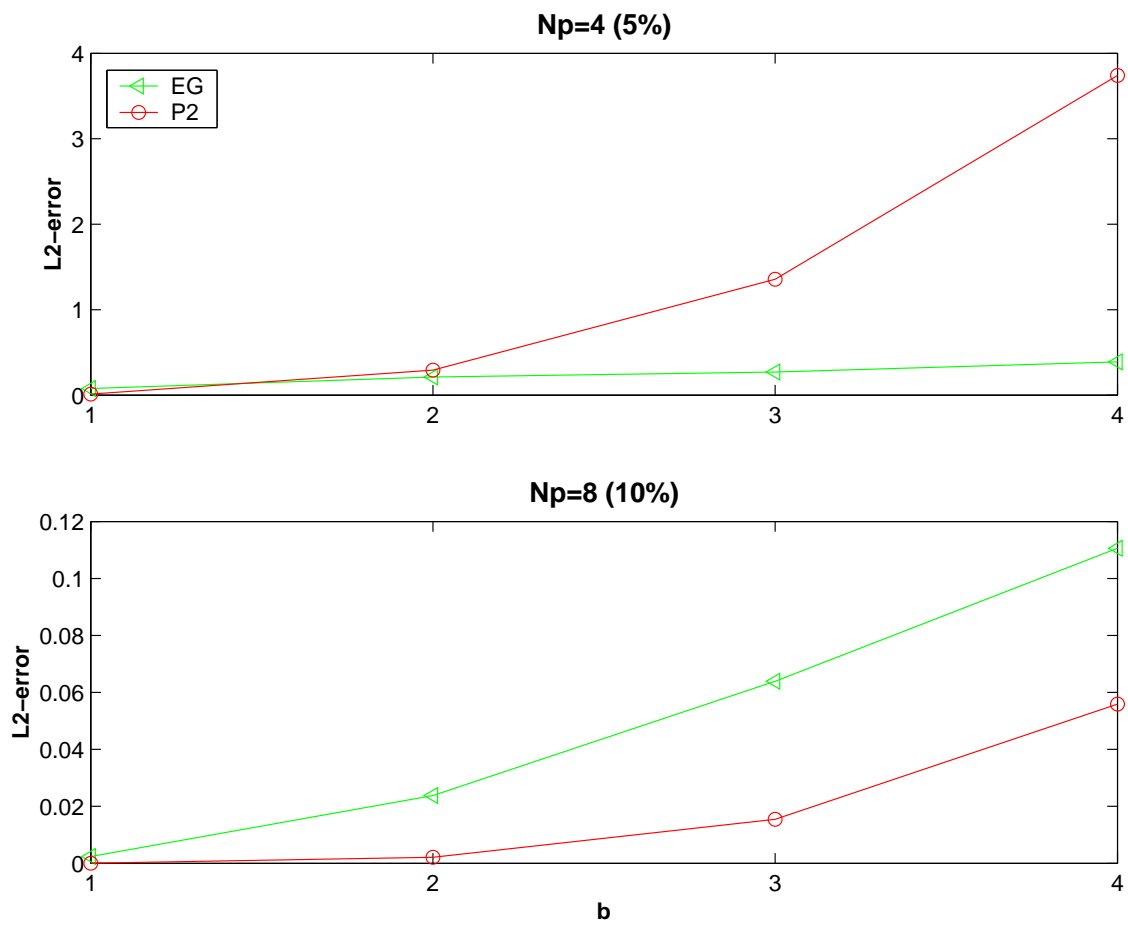


Figure 11: The importance of N_p for the better accuracy of our AIM P2 : The L^2 -errors committed by the Euler-Galerkin method (EG) and the perturbation method with two terms (P2) as a function of the parameter b for Example 2 when $M = 80$ and $T = 40$.

is more costly than P1 and EG. Computational cost for our AIM almost doubles. This is because, when compared with P1 and EG, our AIM P2 includes the derivative of the nonlinear term as well as the nonlinear term itself. In our new method we can add more higher-order terms for even better accuracy under restriction of the smoothness and boundedness of the nonlinear term $F(u)$. But more higher-order terms make for harder implementation, and higher computation costs.

References

- [1] L. Russo, A. Adrover, G. Continillo, Dynamic behavior of a reaction/diffusion system: wavelet-like collocations and approximate inertial manifolds, *COC 2000*, ST.Petersburg, Russia, 2000 IEEE.
- [2] R. Temam, *Infinite-Dimensional Dynamical Systems in Mechanics and Physics*, 2nd ed. Springer Verlag, Berlin, 1988.
- [3] C. Foias, G.R. Sell, R. Temam, Inertial Manifolds for Nonlinear Evolutionary Equations, *J. Differential Equations*, **73**, pp. 309–353, 1988.
- [4] J. Mallet-Paret, G. R. Sell, Inertial manifolds for reaction diffusion equations in higher space dimensions, *J. Amer. Math. Soc.*, **1**, pp. 805–866, 1988.
- [5] M. Marion, Approximate inertial manifolds for reaction-diffusion equations in high space dimension, *J. Dynamics Differential Equations*, **1**, pp. 245–267, 1989.
- [6] C. Foias, O. Manley, R. Temam, Modelling of the interaction of small and large eddies in two dimensional turbulent flows, *Math. Modelling Numer. Anal.*, **22**, pp. 93–118, 1988.
- [7] C. Foias, M.S. Jolly, I.G. Kevrekids, G.R. Sell, E.S. Titi, On the computation of inertial manifolds, *Phys. Lett. A*, **131**, pp. 433–436, 1988.
- [8] C. Foias, G.R. Sell, E.S. Titi, Exponential tracking and approximation of inertial manifolds for dissipative nonlinear equations, *J. Dyn. Differential Equations*, **1**, pp. 199–243, 1989.
- [9] A. Debussche, M. Marion, On the Construction of Families of Approximate Inertial Manifolds, *J. Differential Equations*, **100**, pp. 173–201, 1992.
- [10] Jos L.M. Van Dorsselaer, C. Lubich; Inertial manifolds of parabolic differential equations under higher-order discretizations, *IMA J. Numer. Anal.*, **19**, pp. 455–471, 1999.
- [11] J. Novo, E.S. Titi, S. Wynne; Efficient methods using high accuracy approximate inertial manifolds, *Numer. Math.*, **87**, pp. 523–554, 2001.